

## **Elastodynamic single-sided homogeneous Green's function representation: Theory and examples**

Christian Reinicke Urruticoechea and Kees Wapenaar

### **Summary**

The homogeneous Green's function is the Green's function minus its time-reversal. Many wavefield imaging applications make use of the homogeneous Green's function in form of a closed boundary integral. Wapenaar et al. (2016a) derived an accurate single-sided homogeneous Green's function representation that only requires sources/receivers on an open boundary. In this abstract we will present a numerical example of elastodynamic single-sided homogeneous Green's function representation using a 2D laterally invariant medium. First, we will outline the theory of the single-sided homogeneous Green's function representation. Second, we will show numerical results for the elastodynamic case.

## Introduction

The homogeneous Green's function is the superposition of the Green's function and its time-reversal. For lossless media the Green's function and its time-reversal obey the same wave equation with a delta source. Consequently, the homogenous Green's function obeys the wave equation with a source term equal to zero. Many wavefield imaging applications make use of the homogeneous Green's function in form of a closed boundary integral. In previous work an accurate single-sided homogeneous Green's function representation was derived that only requires sources/receivers on an open boundary (Wapenaar et al., 2016b). This representation is valid for a scalar wavefield and accounts for internal multiple scattering. Subsequently, the theory of single-sided homogeneous Green's function representation was extended to a unified matrix-vector notation for acoustic, quantum-mechanical, electromagnetic and elastodynamic waves (Wapenaar et al., 2016a). We present a numerical example of elastodynamic single-sided homogeneous Green's function representation using a 2D laterally invariant medium. First, we outline the theory of the single-sided homogeneous Green's function representation. Second, we show numerical results for the elastodynamic case.

### Elastodynamic single-sided homogeneous Greens function representation: Theory

We consider power-flux normalised one-way wavefields, i.e. a wavefield quantity  $\mathbf{p}$  is organised in a block matrix;

$$\mathbf{p} = \begin{pmatrix} \mathbf{p}^{++} & \mathbf{p}^{+-} \\ \mathbf{p}^{-+} & \mathbf{p}^{--} \end{pmatrix}; \mathbf{p}^{XY} = \begin{pmatrix} \mathbf{p}_{pp}^{XY} & \mathbf{p}_{ps}^{XY} \\ \mathbf{p}_{sp}^{XY} & \mathbf{p}_{ss}^{XY} \end{pmatrix}; \quad (1)$$

where the superscripts "+" and "-" denote downgoing and upgoing wavefields respectively. In the elastic case each one-way block matrix  $\mathbf{p}^{XY}$  is a two by two matrix with four P- and S-wave components.

Consider a medium which is bounded by an infinite, horizontal, reflection-free boundary  $\partial\mathbb{D}_0$  at the top. The  $x_3$  coordinate is defined as downward pointing. We refer to this medium as the actual medium. Let  $\mathbf{x}_A$  and  $\mathbf{x}_B$  be two points inside the medium. A representation of the homogeneous Green's function  $\mathbf{G}_h(\mathbf{x}_A, \mathbf{x}_B, \omega)$  using reflection data  $\mathbf{R}(\mathbf{x}, \mathbf{x}', \omega)$  recorded at the surface and a so-called focusing function  $\mathbf{F}(\mathbf{x}, \mathbf{x}_A, \omega)$  is given by (Wapenaar et al., 2016a) ;

$$\mathbf{G}_1(\mathbf{x}, \mathbf{x}_B, \omega) = \int_{\partial\mathbb{D}'_0} \mathbf{G}_h(\mathbf{x}, \mathbf{x}', \omega) \mathbf{F}(\mathbf{x}', \mathbf{x}_B, \omega) \mathbf{I}_1^t d^2\mathbf{x}'; \quad (2)$$

$$\mathbf{G}_h(\mathbf{x}, \mathbf{x}_B, \omega) = \mathbf{G}_1(\mathbf{x}, \mathbf{x}_B, \omega) - \mathbf{K} \mathbf{G}_1^*(\mathbf{x}, \mathbf{x}_B, \omega) \mathbf{K}; \quad (3)$$

$$\mathbf{G}_2(\mathbf{x}_A, \mathbf{x}_B, \omega) = \int_{\partial\mathbb{D}_0} \mathbf{I}_2 \mathbf{F}^t(\mathbf{x}, \mathbf{x}_A, \omega) \mathbf{N} \mathbf{G}_h(\mathbf{x}, \mathbf{x}_B, \omega) d^2\mathbf{x}; \quad (4)$$

$$\mathbf{G}_h(\mathbf{x}_A, \mathbf{x}_B, \omega) = \mathbf{G}_2(\mathbf{x}_A, \mathbf{x}_B, \omega) - \mathbf{K} \mathbf{G}_2^*(\mathbf{x}_A, \mathbf{x}_B, \omega) \mathbf{K}. \quad (5)$$

Here the surface  $\partial\mathbb{D}'_0$  is defined just below  $\partial\mathbb{D}_0$ . The matrices  $\mathbf{K}$ ,  $\mathbf{N}$ ,  $\mathbf{I}_1$ , and  $\mathbf{I}_2$  are defined as;

$$\mathbf{K} = \begin{pmatrix} \mathbf{O} & \mathbf{I} \\ \mathbf{I} & \mathbf{O} \end{pmatrix}; \mathbf{N} = \begin{pmatrix} \mathbf{O} & \mathbf{I} \\ -\mathbf{I} & \mathbf{O} \end{pmatrix}; \mathbf{I}_1 = \begin{pmatrix} \mathbf{I} \\ \mathbf{O} \end{pmatrix}; \mathbf{I}_2 = \begin{pmatrix} \mathbf{O} \\ \mathbf{I} \end{pmatrix}; \quad (6)$$

where  $\mathbf{I}$  is an identity matrix and  $\mathbf{O}$  is a zero matrix. The quantities in brackets represent the receiver and source coordinates respectively, the third quantity is the temporal frequency. The homogeneous reflection data  $\mathbf{G}_h(\mathbf{x}, \mathbf{x}', \omega)$  can be built from reflection data  $\mathbf{R}(\mathbf{x}, \mathbf{x}', \omega)$ ;

$$\mathbf{G}_h(\mathbf{x}, \mathbf{x}', \omega) = \mathbf{G}(\mathbf{x}, \mathbf{x}', \omega) - \mathbf{K}\mathbf{G}^*(\mathbf{x}, \mathbf{x}', \omega)\mathbf{K} = \begin{pmatrix} \mathbf{I} & -\mathbf{R}^*(\mathbf{x}, \mathbf{x}', \omega) \\ \mathbf{R}(\mathbf{x}, \mathbf{x}', \omega) & -\mathbf{I} \end{pmatrix}. \quad (7)$$

The focusing function  $\mathbf{F}(\mathbf{x}, \mathbf{x}_A, \omega)$  is defined in a reference medium which is bounded by the reflection-free surface  $\partial\mathbb{D}_0$  at the top and  $x_3 = x_{3,A}$  at the bottom. For  $x_3 \in [0, x_{3,A}]$  the reference medium is identical to the actual medium. The source-term of the focusing function equals zero. The focusing function consists of a downgoing part  $\mathbf{F}^+(\mathbf{x}, \mathbf{x}_A, \omega)$  and an upgoing part  $\mathbf{F}^-(\mathbf{x}, \mathbf{x}_A, \omega)$ . The downgoing focusing function is defined as the inverse of the transmission response,  $\mathbf{T}^+(\mathbf{x}_A, \mathbf{x}, \omega)$ , in the reference medium which is the response of point sources distributed along the surface  $\partial\mathbb{D}_0$  recorded at a receiver placed at  $\mathbf{x}_A$ ;

$$\int_{\partial\mathbb{D}_0} \mathbf{T}^+(\mathbf{x}, \mathbf{x}', \omega) \mathbf{F}^+(\mathbf{x}', \mathbf{x}_A, \omega) d^2\mathbf{x}' = \mathbf{I}\delta(\mathbf{x}_H - \mathbf{x}_{H,A}); \quad (8)$$

for  $x_3 = x_{3,A}$ . The coordinate  $\mathbf{x}_H$  represents the horizontal spatial coordinates  $(x_1, x_2)$ . The upgoing focusing function  $\mathbf{F}^-(\mathbf{x}, \mathbf{x}_A, \omega)$  is defined as the reflection response of the downgoing focusing function in the reference medium. Following the definition of the focusing function one can see that the focusing function obeys a so-called focusing condition;

$$\mathbf{F}(\mathbf{x}, \mathbf{x}_A, \omega) |_{x_3=x_{3,A}} = \begin{pmatrix} \mathbf{F}^+ \\ \mathbf{F}^- \end{pmatrix}(\mathbf{x}, \mathbf{x}_A, \omega) = \begin{pmatrix} \mathbf{I}\delta(\mathbf{x}_H - \mathbf{x}_{H,A}) \\ \mathbf{O} \end{pmatrix}. \quad (9)$$

The physical interpretation of this condition is that when the focusing function is injected into the medium at the surface  $\partial\mathbb{D}_0$  it focuses at the point  $\mathbf{x}_A$ . By applying an inverse Fourier transform to equation 9 one can see that in the time domain the focusing function also focuses in time at  $t = 0$ s. Figure 1a illustrates the focusing function.

Equations 2 - 5 consist of two steps. First, the source of the reflection data is redatumed to  $\mathbf{x}_B$ , i.e. a virtual source is created inside the medium. The causal part of the resulting homogeneous Green's function  $\mathbf{G}_h(\mathbf{x}, \mathbf{x}_B, \omega)$  is sketched in Figure 1b. Second, the receivers are redatumed from the surface to  $\mathbf{x}_A$ , i.e. a virtual receiver is created inside the medium resulting in the homogeneous Green's function  $\mathbf{G}_h(\mathbf{x}_A, \mathbf{x}_B, \omega)$  (see Figure 1b).

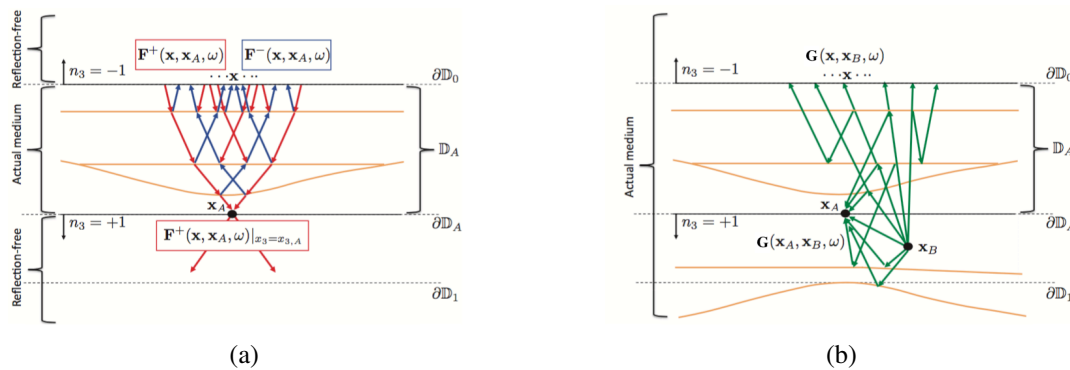


Figure 1: Sketch of (a) the downgoing and upgoing focusing functions  $\mathbf{F}^\pm(\mathbf{x}, \mathbf{x}_A, \omega)$ , (b) the Green's functions  $\mathbf{G}(\mathbf{x}, \mathbf{x}_B, \omega)$  and  $\mathbf{G}(\mathbf{x}_A, \mathbf{x}_B, \omega)$ .

## Elastodynamic single-sided homogeneous Greens function representation: Examples

We present a numerical example of elastodynamic single-sided homogeneous Green's function representation following the theory shown above. This example is a feasibility test using the 2D lossless model shown in Figure 2a. The model has three density contrasts and constant P- and S-wave velocities,  $c_P = 2500 \text{ m s}^{-1}$ ,  $c_S = 2000 \text{ m s}^{-1}$ . Note that the example works equally well with non-constant velocities. The spatial coordinates are denoted by  $(x_1, x_3)$ . Since the model is laterally invariant all of the above equations can be transformed to the horizontal wavenumber ( $k_1$ ) domain using Plancherel's theorem;

$$\int_{-\infty}^{\infty} g^*(x_1) f(x_1) dx_1 = \frac{1}{2\pi} \int_{-\infty}^{\infty} \tilde{g}^*(k_1) \tilde{f}(k_1) dk_1. \quad (10)$$

Therefore, we use a wavefield extrapolation code which models each horizontal wavenumber  $k_1$  separately. First, the focusing function is convolved with the homogeneous reflection data to create a virtual source inside the medium. Bear in mind that in the horizontal wavenumber domain the convolution is a multiplication. Here we created a virtual source at  $\mathbf{x}_B = (x_1 = 0 \text{ m}, x_3 = 2000 \text{ m})$ . The resulting wavefield,  $\mathbf{G}_h(\mathbf{x}, \mathbf{x}_B, t)$ , is the impulse response of a point source located at the virtual source position  $\mathbf{x}_B$  and recorded at the surface  $\partial\mathbb{D}_0$  combined with its time-reversal. Figure 2b shows the homogeneous Green's function  $\mathbf{G}_h(\mathbf{x}, \mathbf{x}_B, t)$  after applying a 2D inverse Fourier transform. To illustrate that the presented method accounts for converted as well as multiply scattered waves we highlighted three reflection events in Figure 2b and sketched their corresponding raypaths as a cartoon in Figure 2a. Note that all one-way and P- and S- components of the wavefield are still power-flux normalised.

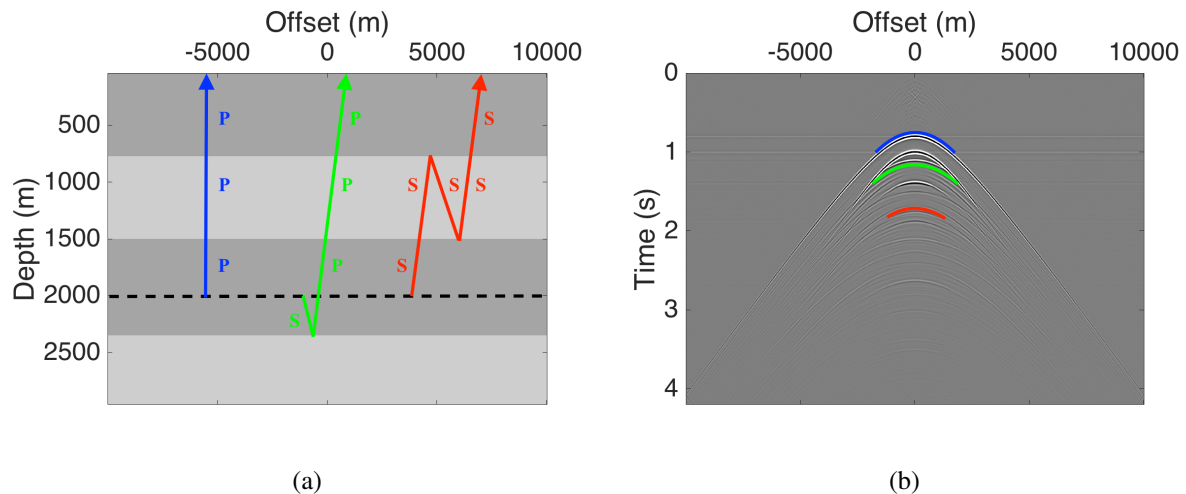


Figure 2: (a) Model: Densities of  $1000 \text{ kg m}^{-3}$  and  $2000 \text{ kg m}^{-3}$  are displayed in dark and light grey respectively. P- and S-wave velocities are constant,  $c_P = 2500 \text{ m s}^{-1}$ ,  $c_S = 2000 \text{ m s}^{-1}$ . (b) Causal part of the elastic homogeneous Green's function  $\mathbf{G}_h(\mathbf{x}, \mathbf{x}_B, t)$  with a virtual source at  $\mathbf{x}_B$ . The events highlighted in colours are sketched as a cartoon in the density model.

Second, the focusing function is used to redatum the receivers from the surface  $\partial\mathbb{D}_0$  to a desired depth level, i.e. virtual receivers are created inside the medium. In this example, a grid of virtual receivers with a horizontal spacing of 12.5 m and a vertical spacing of 20 m is created inside the medium. Since the homogeneous Green's function is an impulse response combined with its time-reversal the represented wavefield is propagating inward at negative times, zero at time zero, and propagating outward from the virtual source location at positive times. Figure 3 shows snapshots of the homogeneous Green's function  $\mathbf{G}_h(\mathbf{x}_A, \mathbf{x}_B, t)$  at positive times. To illustrate that the wavefield in Figure 3 contains P- and S-waves we indicated an upgoing P-wave by a blue line and an upgoing S-wave by a red line. As expected the two indicated waves propagate with different velocities.

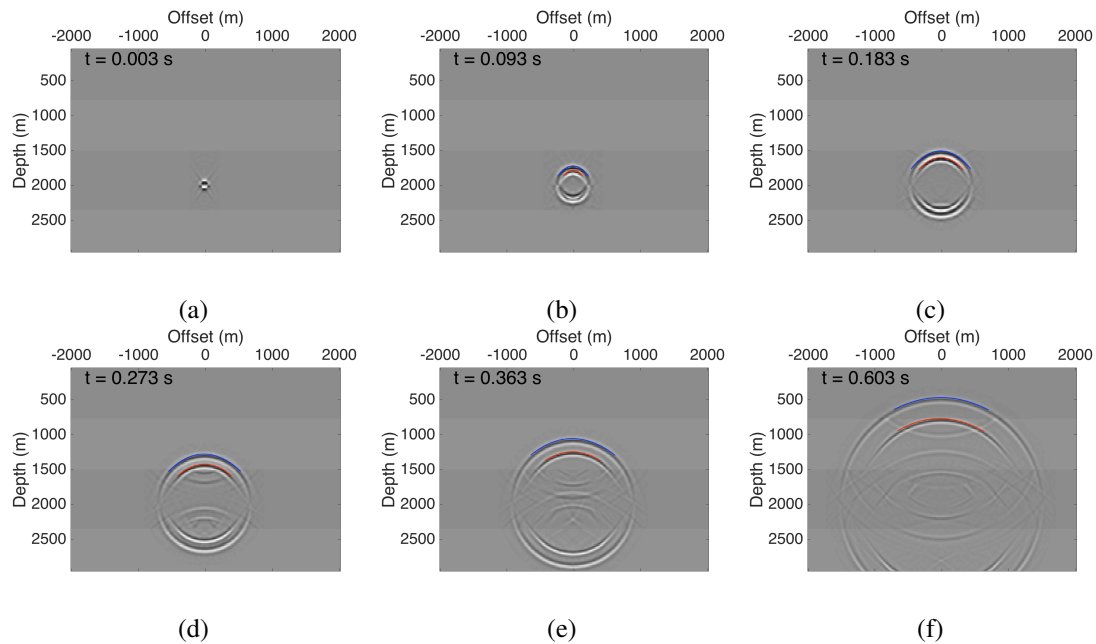


Figure 3: Snapshots of the represented homogeneous Green's function  $\mathbf{G}_h(\mathbf{x}_A, \mathbf{x}_B, t)$  as it propagates from the virtual source  $\mathbf{x}_B$  through the medium. The blue and red lines mark an upgoing P-wave and an upgoing S-wave respectively.

## Discussion and conclusions

We presented a numerical example that demonstrates single-sided homogeneous Green's function representation for elastic waves. Note that the representation accounts for converted as well as multiply scattered waves. We considered a laterally invariant model but we would like to emphasise that the theory is valid for laterally varying media. For the near future we plan to extend the presented numerical example to laterally variant media using a finite difference code. Here, we modelled the focusing functions which is not practical because the modelling requires full knowledge of the medium. In practice, the focusing function should be retrieved using limited knowledge of the medium which is possible using the Marchenko method - Wapenaar (2014) and da Costa Filho et al. (2014). We plan to develop the elastic Marchenko method further to minimise the required knowledge of the medium.

## Acknowledgements

The authors would like to thank the European Marie Curie Initial Training Network WAVES for funding this research project.

## References

- da Costa Filho, C.A., Ravasi, M., Curtis, A. and Meles, G.A. [2014] Elastodynamic Green's function retrieval through single-sided Marchenko inverse scattering. *Physical Review E*, **90**(6), 063201.
- Wapenaar, K. [2014] Single-sided Marchenko focusing of compressional and shear waves. *Physical Review E*, **90**(6), 063202.
- Wapenaar, K., van der Neut, J. and Slob, E. [2016a] Unified double- and single-sided homogeneous Green's function representations. In: *Proc. R. Soc. A*, 472. The Royal Society, 20160162.
- Wapenaar, K., Thorbecke, J. and van der Neut, J. [2016b] A single-sided homogeneous Green's function representation for holographic imaging, inverse scattering, time-reversal acoustics and interferometric Green's function retrieval. *Geophysical Journal International*, **205**(1), 531–535.